PRESSURE DISTRIBUTION ACTING ON BREAKWATER CAISSON UNDER TSUNAMI OVERFLOW
by

Kojiro Suzuki[1] and Kenichiro Shimosako[2]

ABSTRACT

Many caissons of breakwaters were slid or overturned due to tsunami overflow pressure caused by 2011 Tohoku earthquake. To prevent this sliding failure, the pressure estimation method under tsunami overflow was introduced in the new Tsunami-Resistant Design Guideline for Breakwater in 2015. In this guideline, the uplift and the overburden pressure are not considered, instead only static buoyancy acting on the caisson is considered. However, under tsunami overflow, the pressure difference between the bottom and the top of breakwater caisson, especially the caisson having a large parapet, can be extremely larger than the buoyancy force. In order to examine this excess uplift force, a series of hydraulic experiments and numerical simulations were conducted. The experiment was conducted in an experimental flume in which the large pump was installed to produce tsunami overflow. Through the experiments and numerical simulations, it was clarified that the large uplift pressure and the small overburden pressure cause the dynamic buoyancy larger than the quasi-static buoyancy estimated by the design guideline. This upward force reduces the stability of caisson, especially the caisson having the large parapet.

1. INTRODUCTION

The caissons of many breakwaters either slid or overturned due to overflow pressure of the tsunami triggered by the 2011 Tohoku earthquake. For example, the offshore tsunami breakwater of Kamaishi Port, constructed to protect Kamaishi City, was destroyed by the huge tsunami overflowing the breakwater. Up until the 2011 disaster, tsunami overflow had not been considered in breakwater design; rather, it had been estimated by Tanimoto's tsunami force formula *(1)-(4)* (Tanimoto et al., 1984). However, Tanimoto's formula cannot express the force of tsunami overflow.

$$\eta^* = 3.0a_I \qquad (1)$$

$$p_1 = 2.2\rho_0 g a_I \qquad (2)$$

$$p_u = p_1 \qquad (3)$$

$$p_L = p_2 \qquad (4)$$

Since the widespread damage engendered by the Tohoku tsunami overflow, the pressure formula under tsunami overflow has been studied using hydraulic experiments, and, in 2015, the experimental results were introduced in the Tsunami-Resistant Design Guideline for Breakwater (MLIT, 2015). In the guideline, the new tsunami pressure formula is expressed by the quasi-hydrostatic pressure due to the tsunami water level. The front and the rear pressure are expressed as modified hydrostatic pressures *(5)-(7)*. The modification factor is 1.05 at the front (α_f) and 0.9 at the rear (α_r).

$$p_1 = \alpha_f \rho_0 g(\eta_f + h') \qquad (5)$$

$$p_3 = \alpha_r \rho_0 g(\eta_r + h') \qquad (6)$$

_____

[1] Maritime Structures Group, Port and Airport Research Institute, suzuki_k@pari.go.jp
[2] Senior Director for International Affairs, Port and Airport Research Institute

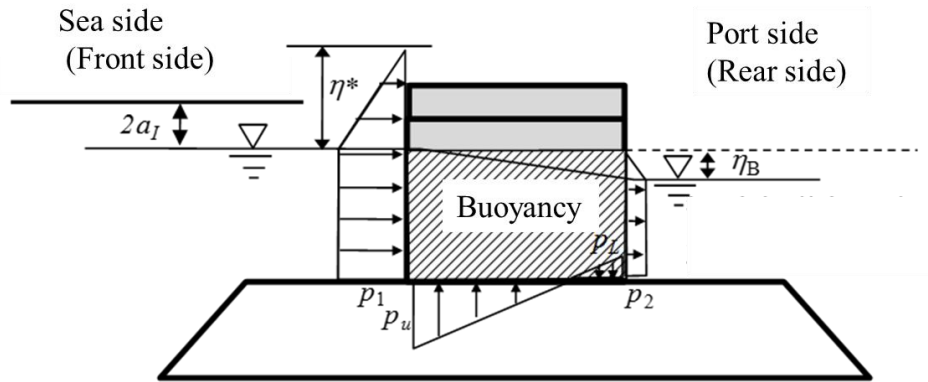$$p_2 = (\eta_f - h_c)/(\eta_f + h')p_1 \qquad\qquad (7)$$

Figure 1: Tanimoto's tsunami pressure distribution (expressed as hydrodynamic pressure)
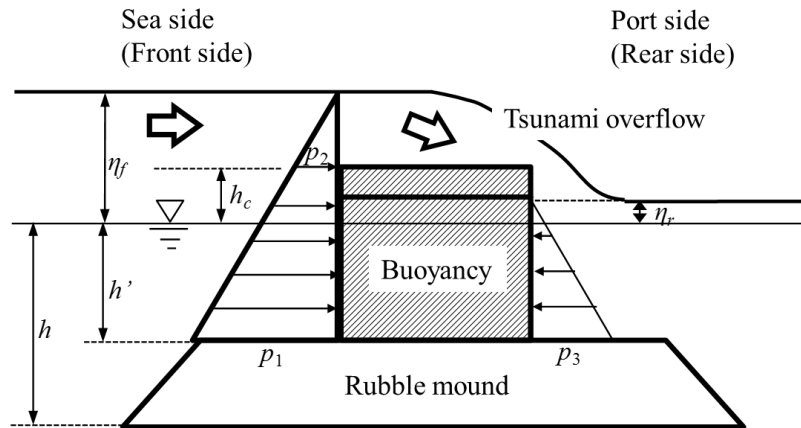

Figure 2: Pressure distribution and buoyancy defined by the Tsunami-Resistant Design Guideline for Breakwater (2015) (expressed as quasi-hydrostatic pressure)

Many breakwaters in Japan have been inspected and redesigned using the new design formula. However, some design problems remain. Because the new design formula is intended for simple rectangular caisson-type breakwaters, the uplift and overburden pressure are not considered; instead, only the buoyancy acting on the caisson is considered in the guideline. However, the buoyancy under hydrostatic condition can be different from the buoyancy under hydrodynamic tsunami condition as shown in the schematic figure (Fig. 3).

In the hydrostatic condition, the buoyancy is equivalent to the weight of the fluid that would otherwise occupy the volume of the object, i.e. the displaced fluid (Fig. 3 (a), (c)). The buoyancy is equivalent to the pressure difference between the bottom and the top of the immersed object. However, under tsunami overflow condition, the pressure difference between the bottom and the top of the breakwater caisson, especially a caisson having a large parapet, can be extremely larger than the buoyancy under hydrostatic condition (Fig. 3 (b), (d)). Here, we define the buoyancy under static condition (tsunami dynamic condition) as static buoyancy, B_{static} (dynamic buoyancy, $B_{dynamic}$).

Sato et al. (2016) estimated the overburden pressure p_o as a trapezoidal pressure distribution. However, the shape of the water surface elevation at the top of caisson isn't a trapezoidal shape while the flow changes from subcritical flow to supercritical flow. Moreover, if the parapet is high and thin and overflow depth is small, mass of displaced fluid can be extremely less than the uplift pressure.

In order to examine this buoyancy, a series of hydraulic experiments and numerical simulations were conducted in this study.
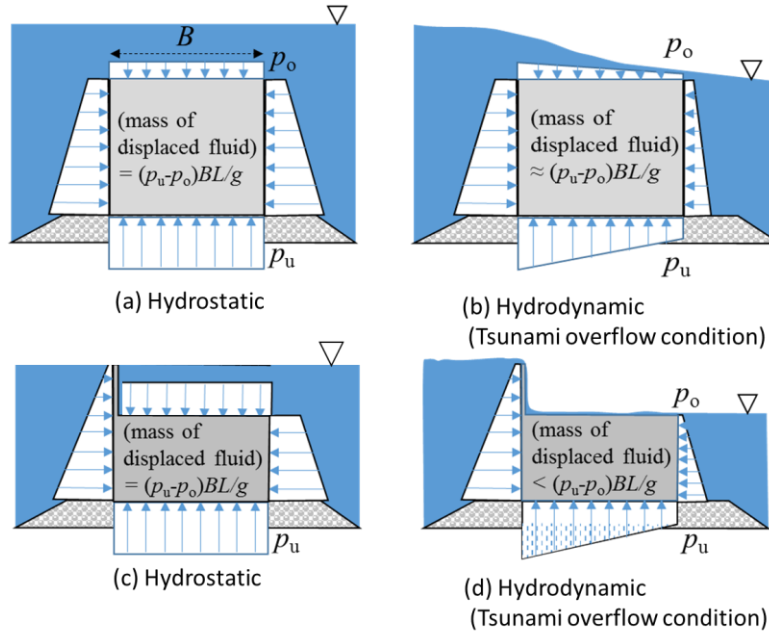

Figure 3: Schematics of buoyancy and pressure distribution under static and dynamic overflow condition. B (L) is the width (length) of the caisson.
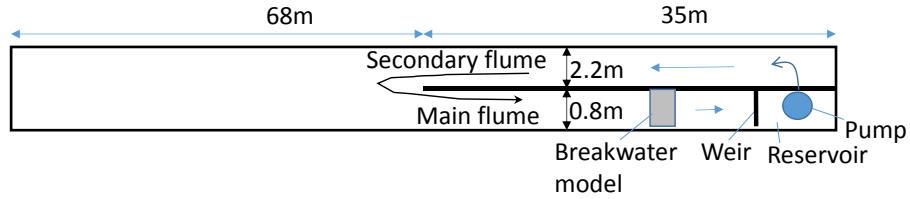
2. HYDRAULIC EXPERIMENT

2.1   Experimental Setup and Condition

The experiments were performed using a flume with the length of 105m. As shown in Fig. 4, the flume was separated by the vertical wall and the width of the main flume and the sub-flume, for circulation of the water, were set to 0.8m and 2.2m, respectively. As shown in Fig. 4, tsunami overflowing on a breakwater model was reproduced under uniform flow, which was generated by a pump installed behind a weir in the main flume, and circulated through the main and secondary flumes. Pressure gauges, water elevation gauges and propeller-type current profilers were installed around breakwater model.

Initial water depth h_f (inundation depth η_f) was changed from 0.42 to 0.52m (from 0.044 to 0.144m). The height of weir was changed from 0.14 to 0.35m.
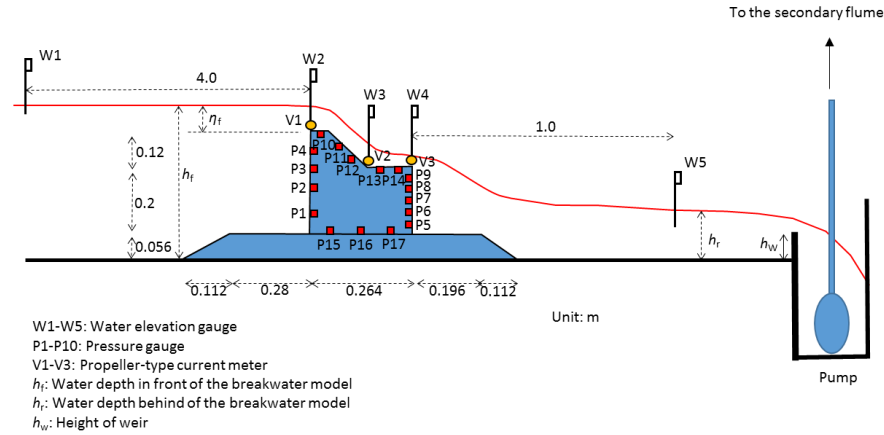
(a) Plan view

(b) Sectional view

W1-W5: Water elevation gauge
P1-P10: Pressure gauge
V1-V3: Propeller-type current meter
h_f: Water depth in front of the breakwater model
h_r: Water depth behind of the breakwater model
h_w: Height of weir

Figure 4: Details of the experimental flume and the model

2.2   Experimental Results

Fig. 5 shows the pressure distribution around the caisson under overflow condition. The pressure distribution in front and behind the caisson is almost static and triangle shape. In contrast, the pressure on the caisson is different from the pressure distribution estimated from the water surface elevation. The pressure at the front part (rear part) of the top of caisson measured by the pressure gauges is smaller (larger) than the pressure estimated from the water surface elevation. Decrease of pressure at the front part is supposed to be caused by the increase of velocity, the significant downward acceleration of the water particle around the curving flow and the occurrence of eddy. On the other hand, increase of pressure at the rear part is supposed to be caused by the collision of water on the caisson.

Fig. 6 shows the relationship between the velocity (V1) and the pressure decrease, Δp (P10) at the top of the caisson. The pressure is nondimensionalized by the water depth, η at P10. Pressure decreases as the velocity increases. The pressure decrease is supposed to be caused by the increase of velocity and the significant downward acceleration of the water particle around the curving flow
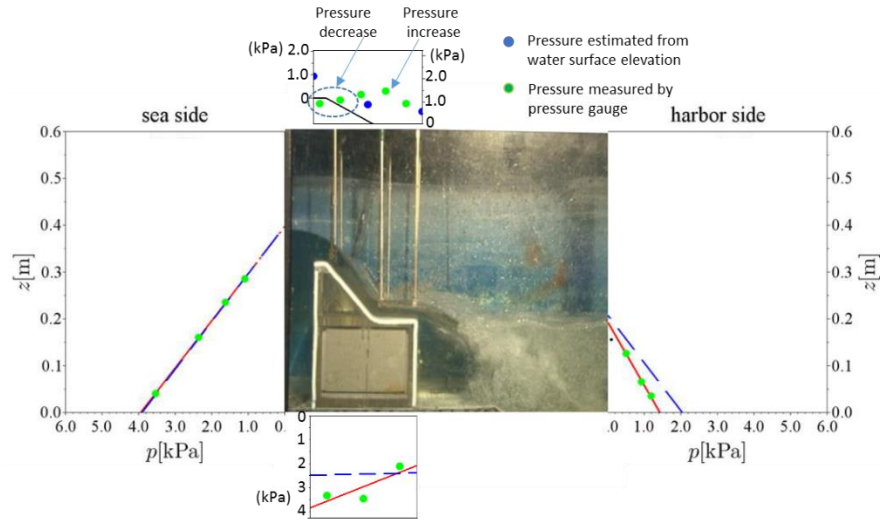
4

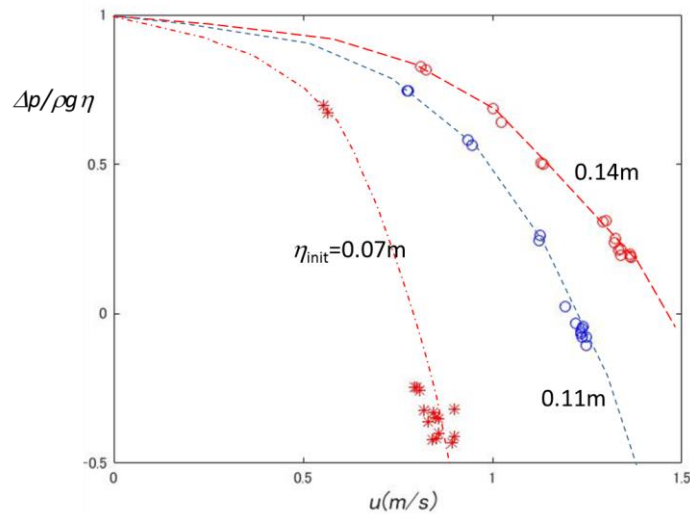**Figure 5: Pressure distribution on top of the caisson**

Figure 6: Relationship between velocity and pressure decrease at the top of the caisson

3. NUMERICAL ANALYSIS

3.1   Computation method

Tsunami overflow reproduced in the hydraulic experiment was simulated by the VOF method implemented in the CADMAS-SURF-2D CFD model (CDIT, 2001). Fig.7 shows the schematic of the computation domain and boundary condition. Inflow (Outflow) velocity is set as 0.02-0.1m/s (0.3m/s) at the offshore (onshore) boundary. The horizontal and vertical grid size is 0.01m. The initial water depth was set at 0.39-0.45m. The weir set the water level behind the caisson and the height was 0.14 and 0.2m.

Four caisson models were examined as shown in Fig. 8. Cross section 1 (CS1) corresponds to the caisson model of the experiment.
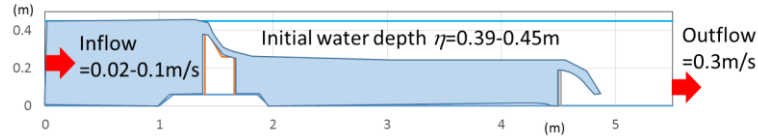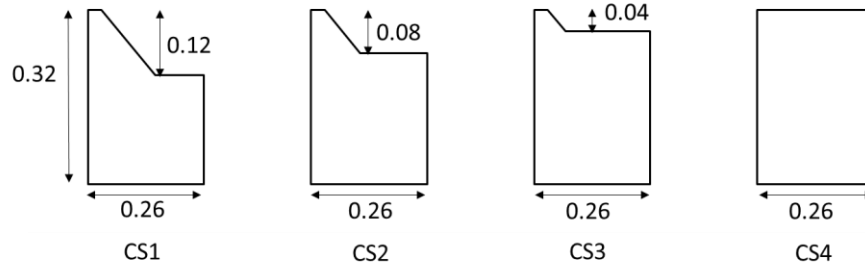
Figure 7: shows the cross section of numerical

Figure 8: Cross sections of caisson model

3.2   Computation Result

Fig.9 shows the snapshot of the CS1. The water surface elevation in front of caisson is 0.45m and the height of the weir behind the caisson is 0.2m.

Fig.10 shows the pressure at the top and bottom of the caisson (p_{bottom}, p_{top}) with water surface elevation ($h_{surface}$). Pressure head ($p_{top}/\rho g$) at the front part of the top of caisson is smaller than the water surface elevation ($h_{surface}$) as shown in the experimental result (Fig.5).

Fig.11 shows the ratio of dynamic buoyancy ($B_{dynamic}$) and static buoyancy (B_{static}) with different water surface elevation ($\eta_{front}/h_{caisson}$) when the height of weir (h_{weir}) is 0.14m. Here, η_{front} is defined as water surface elevation in front of caisson during tsunami overflow and $h_{caisson}$ is the caisson height. Since the water depth behind the caisson is shallow, the pressure at the bottom of the caisson is small, resulting the dynamic buoyancy ($B_{dynamic}$) is smaller than the static buoyancy (B_{static}).

In contrast, the ratio of Fig.12 is much larger than the ratio of Fig.11 when the height of weir (h_{weir}) is 0.2m. In the case of CS1 and CS2 (Caisson with large parapet), the dynamic buoyancy ($B_{dynamic}$) is 5% larger than the static buoyancy (B_{static}).
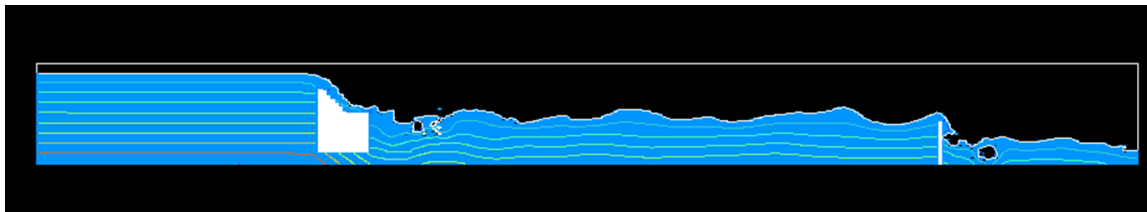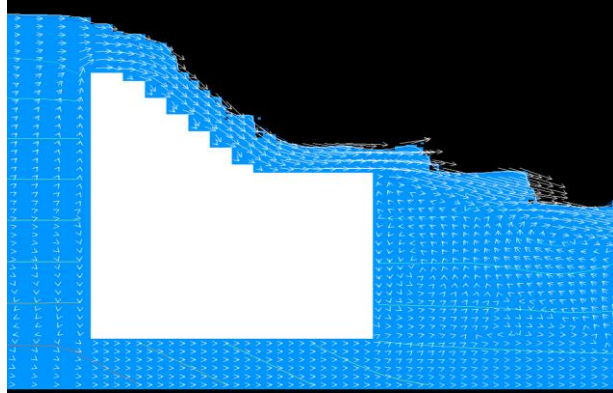
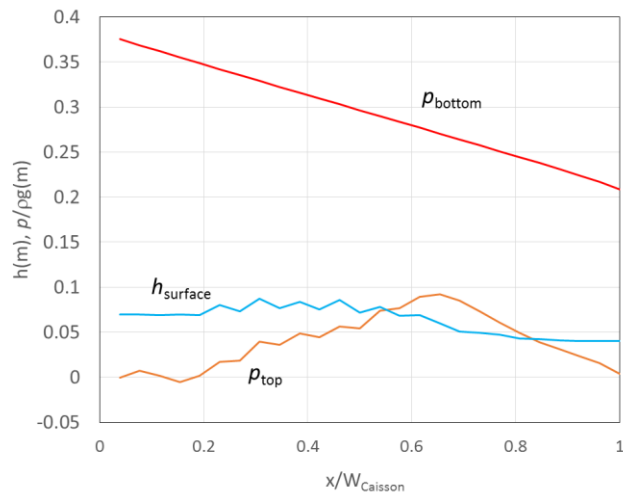Figure 9: Snapshot of CS1 (h_{front}=0.45m, h_{weir}=0.2m)

Figure 10: Pressure at bottom and top of the caisson (p_{bottom}, p_{top}) with water surface elevation ($h_{surface}$) (CS1, h_{front}=0.45m, h_{weir}=0.2m)
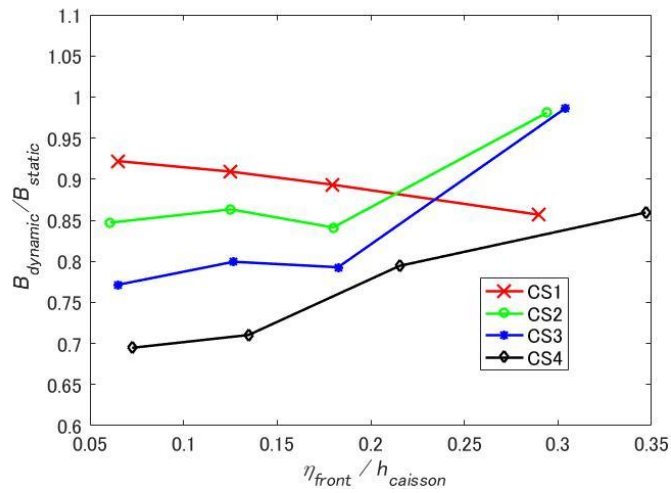

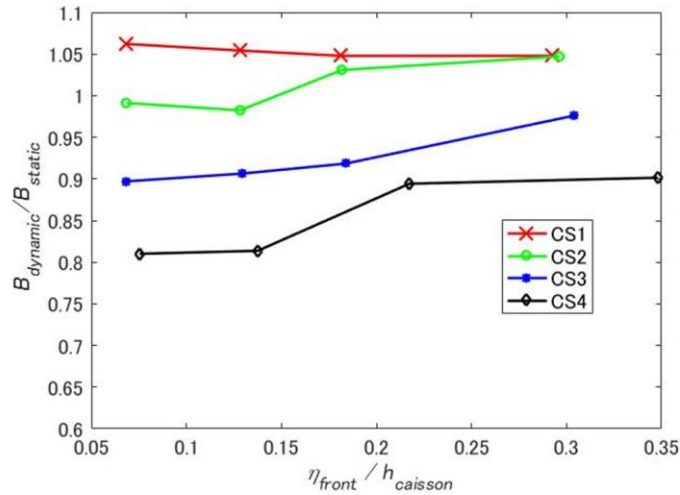Figure 11: Ratio of dynamic and static buoyancy (h_{weir}=0.14m)

Figure 12: Ratio of dynamic and static buoyancy (h_{weir}=0.2m)

4.   CONCLUSIONS

A hydraulic experiment and a numerical simulation of tsunami overflowing on the caisson type breakwater was conducted and the following clarified.

1) The pressure on the caisson under tsunami overflow condition is smaller than the static water pressure corresponding to the water level. The significant downward acceleration of the water particle around the curving flow appears to be the main reasons of the observed pressure drop at the front end of the caisson.
2) The large uplift pressure and the small overburden pressure during tsunami overflow cause the large dynamic buoyancy. The dynamic buoyancy acting on the caisson with large parapet is 5% larger than the static buoyancy estimated by the design guideline (2015).

References

Coastal development institute of technology (CDIT) (2001). CADMAS-SURF, CDIT library No. 12, 68p.

Ministry of Land, Infrastructre, Transport and Tourism (MLIT) (2015). Tsunami-Resistant Design Guideline for Breakwater, website; http://www.mlit.go.jp/kowan/kowan_tk5_000018.html. (in Japanese).

Sato, M., Omura, A., Shibata, D., Uehara, K., Oikawa, T., & Aoki, N. (2016). Analysis on the Effect of Widening Works of Breakwaters against Tsunami-induced Seepage Flow in the Rubble Mound, Journal of Japan Society of Civil Engineers, Ser. B3 (Ocean Engineering), Vol.72, No.2, pp.I_533-I_538. (in Japanese).

Tanimoto, K., Tsuruya, H. and Nakano, S. (1984). Experimental Study of Tsunami Force and Investigation of the Cause of Sea Wall Damage During 1983 Nihonkai Chubu Earthquake, Proc.31st Japanese Conf. Coastal Eng., pp.257-261. (in Japanese)